

## DYNAMICS OF cD CLUSTERS OF GALAXIES. IV. CONCLUSION OF A SURVEY OF 25 ABELL CLUSTERS

WILLIAM R. OEGERLE<sup>1,2</sup> AND JOHN M. HILL<sup>3</sup>

*Received 2000 October 29; accepted 2001 July 25*

### ABSTRACT

We present the final results of a spectroscopic study of a sample of cD galaxy clusters. The goal of this program has been to study the dynamics of the clusters, with emphasis on determining the nature and frequency of cD galaxies with peculiar velocities. Redshifts measured with the MX Spectrometer have been combined with those obtained from the literature to obtain typically 50–150 observed velocities in each of 25 galaxy clusters containing a central cD galaxy. We present a dynamical analysis of the final 11 clusters to be observed in this sample. All 25 clusters are analyzed in a uniform manner to test for the presence of substructure and to determine peculiar velocities and their statistical significance for the central cD galaxy. These peculiar velocities were used to determine whether or not the central cD galaxy is at rest in the cluster potential well. We find that 30%–50% of the clusters in our sample possess significant subclustering (depending on the cluster radius used in the analysis), which is in agreement with other studies of non-cD clusters. Hence, the dynamical state of cD clusters is not different than that of other present-day clusters. After careful study, four of the clusters appear to have a cD galaxy with a significant peculiar velocity. Dressler-Shectman tests indicate that three of these four clusters have statistically significant substructure within  $1.5 h_{75}^{-1}$  Mpc of the cluster center. The dispersion of the cD peculiar velocities is  $164_{-34}^{+41}$  km s<sup>-1</sup> around the mean cluster velocity. This represents a significant detection of peculiar cD velocities but at a level that is far below the mean velocity dispersion for this sample of clusters. The picture that emerges is one in which cD galaxies are nearly at rest with respect to the cluster potential well but have small residual velocities due to subcluster mergers.

*Key words:* galaxies: clusters: general — galaxies: clusters: individual (A779, A1691, A1749, A1767, A1837, A1927, A2061, A2067, A2079, A2089, A2199, A2666) — galaxies: elliptical and lenticular, cD — galaxies: kinematics and dynamics

### 1. INTRODUCTION

First-ranked elliptical galaxies in clusters, also referred to as brightest cluster galaxies (BCGs), are the brightest and most massive galaxies in the universe. About 20% of BCGs are surrounded by large low surface brightness envelopes and are called cD galaxies. cDs exist only in clusters and groups and never in the field. Their existence and evolution are intimately tied to the formation and evolution of the clusters themselves. Although a wealth of data on the properties of cD galaxies exists, it is still unknown whether cDs are the products of dynamical processes operating in clusters prior to their collapse or after cluster virialization.

Clues to the formation of cD galaxies may be found in kinematic studies of cDs and their parent clusters. The properties of cD galaxies are generally consistent with the galaxy lying at the bottom of the cluster potential well. They are located at cluster centers (Matthews, Morgan, & Schmidt 1964) and they are located at the peak of the cluster X-ray emission (Jones et al. 1979). Quintana & Lawrie (1982) investigated the kinematics of nine cD clusters and concluded that all the cD galaxies in their sample were at rest with respect to their parent clusters within the observational uncertainties. More recent work with better determination of velocity distributions has revealed several

cases in which a cD galaxy has a statistically significant peculiar velocity with respect to its parent cluster (Sharples, Ellis, & Gray 1988; Hill et al. 1988; Oegerle & Hill 1994).

In the “cannibalism” model of cD formation, large galaxies at the center of a cluster merge to form a cD, which then continues to grow through accretion of cluster galaxies (Hausman & Ostriker 1978). If these mergers happened long ago, then dynamical friction should have settled the cD galaxy to rest at the bottom of the cluster potential well. However, strong cannibalization seems to have been ruled out by the observational studies of Lauer (1988), who concludes that this mechanism cannot solely account for the large luminosity ( $\sim 10L^*$ ) of cD galaxies. Merritt (1985) argued that the tidal field in clusters will disrupt galaxy halos, thereby lengthening the dynamical friction timescale and acting to diminish cannibalism. Merritt proposed that cDs are formed early in the life of a cluster and that the cD must form at the dynamical center of the cluster to avoid tidal truncation of its envelope. Dubinski (1998) has simulated the formation of a cluster in a hierarchical cosmological model and shown that a BCG will form early in the cluster’s history at the cluster center through the mergers of several massive galaxies flowing inward along filaments. The photometric and internal kinematic properties of the simulated BCG bear a striking resemblance to the observed properties of real BCGs, although the simulation did not produce the extended low surface brightness envelopes associated with cD galaxies. This simulation was carried out with initial conditions that led to a fairly poor cluster at the present epoch (59 galaxies) and did not include the possible effects of subcluster mergers that one might expect in the hierarchical formation of a rich cluster.

<sup>1</sup> Department of Physics and Astronomy, Johns Hopkins University, 3400 North Charles Street, Baltimore, MD 21218-2686.

<sup>2</sup> Current address: Laboratory for Astronomy and Solar Physics, Code 681, Goddard Space Flight Center, Greenbelt, MD 20771; william.oegerle@gsfc.nasa.gov.

<sup>3</sup> Steward Observatory, University of Arizona, 933 North Cherry Avenue, Tucson, AZ 85721-0065; jhill@as.arizona.edu.

TABLE 1  
cD CLUSTER VELOCITIES AND DISPERSIONS

Cluster (1)	$N_{\text{obs}}$ (2)	$N_{\text{cl}}$ (3)	$N_{\text{bi}}$ (4)	$\bar{v}$ (5)	$C_{\text{bi}}$ (6)	$\sigma$ (7)	$S_{\text{bi}}$ (8)
A85 .....	172	130	136	$16,507 \pm 102$	$16,578 \pm 100$	$1097^{+76}_{-63}$	$1166^{+80}_{-67}$
	138	108	113	$16,486 \pm 116$	$16,560 \pm 114$	$1138^{+87}_{-71}$	$1211^{+92}_{-75}$
A193 .....	103	75	78	$14,566 \pm 87$	$14,592 \pm 90$	$717^{+67}_{-53}$	$797^{+75}_{-59}$
	82	72	75	$14,566 \pm 88$	$14,590 \pm 81$	$708^{+68}_{-53}$	$787^{+76}_{-59}$
A399 .....	94	92	92	$21,527 \pm 132$	$21,535 \pm 127$	$1178^{+98}_{-79}$	$1220^{+102}_{-81}$
	78	76	76	$21,437 \pm 148$	$21,420 \pm 143$	$1205^{+112}_{-88}$	$1244^{+116}_{-90}$
A401 .....	133	122	122	$22,084 \pm 108$	$22,050 \pm 102$	$1111^{+79}_{-65}$	$1124^{+80}_{-66}$
	101	94	94	$22,098 \pm 130$	$22,057 \pm 123$	$1170^{+96}_{-77}$	$1189^{+98}_{-79}$
A779 .....	114	83	83	$6,742 \pm 253$	$6,872 \pm 81$	$2256^{+199}_{-157}$	$741^{+65}_{-52}$
	89	53	64	$6,812 \pm 54$	$6,845 \pm 64$	$379^{+44}_{-33}$	$512^{+59}_{-44}$
A1651 .....	45	37	39	$25,322 \pm 171$	$25,284 \pm 175$	$943^{+134}_{-94}$	$1094^{+156}_{-109}$
	35	32	33	$25,306 \pm 184$	$25,277 \pm 182$	$945^{+147}_{-100}$	$1048^{+163}_{-111}$
A1691 .....	82	70	71	$21,613 \pm 96$	$21,637 \pm 91$	$751^{+73}_{-57}$	$765^{+74}_{-58}$
	65	59	59	$21,668 \pm 107$	$21,686 \pm 97$	$751^{+81}_{-61}$	$748^{+80}_{-61}$
A1749 .....	69	51	53	$17,173 \pm 158$	$16,800 \pm 109$	$1048^{+123}_{-91}$	$791^{+93}_{-69}$
	68	51	53	$17,173 \pm 158$	$16,800 \pm 109$	$1048^{+123}_{-91}$	$791^{+93}_{-69}$
A1767 .....	64	59	59	$21,076 \pm 119$	$21,125 \pm 109$	$842^{+91}_{-69}$	$838^{+90}_{-68}$
	59	57	57	$21,077 \pm 123$	$21,128 \pm 113$	$856^{+94}_{-71}$	$856^{+94}_{-71}$
A1795 .....	115	97	102	$18,730 \pm 88$	$18,772 \pm 92$	$806^{+65}_{-53}$	$926^{+75}_{-61}$
	105	91	96	$18,723 \pm 93$	$18,773 \pm 99$	$827^{+70}_{-56}$	$966^{+81}_{-65}$
A1809 .....	62	54	55	$23,721 \pm 111$	$23,702 \pm 105$	$740^{+84}_{-63}$	$777^{+88}_{-66}$
	52	47	47	$23,757 \pm 123$	$23,742 \pm 113$	$766^{+95}_{-70}$	$776^{+96}_{-70}$
A1837 .....	65	32	38	$20,985 \pm 123$	$20,941 \pm 156$	$636^{+99}_{-68}$	$958^{+149}_{-102}$
	46	30	34	$20,956 \pm 129$	$20,930 \pm 139$	$647^{+105}_{-71}$	$811^{+132}_{-89}$
A1927 .....	76	48	59	$28,413 \pm 98$	$28,421 \pm 106$	$608^{+74}_{-54}$	$814^{+99}_{-73}$
	43	36	36	$29,009 \pm 424$	$28,556 \pm 243$	$2276^{+229}_{-229}$	$1460^{+211}_{-147}$
A2029 .....	90	85	86	$23,168 \pm 168$	$23,120 \pm 159$	$1436^{+125}_{-99}$	$1470^{+128}_{-102}$
	83	80	81	$23,150 \pm 175$	$23,096 \pm 165$	$1453^{+131}_{-103}$	$1489^{+134}_{-106}$
A2052 .....	96	73	77	$10,640 \pm 90$	$10,561 \pm 89$	$736^{+70}_{-55}$	$777^{+74}_{-58}$
	71	60	62	$10,611 \pm 83$	$10,593 \pm 79$	$596^{+64}_{-49}$	$621^{+67}_{-51}$
A2063 .....	95	79	80	$10,474 \pm 78$	$10,485 \pm 77$	$660^{+60}_{-48}$	$686^{+63}_{-49}$
	70	63	63	$10,532 \pm 93$	$10,564 \pm 90$	$695^{+72}_{-55}$	$712^{+74}_{-57}$
A2067 .....	79	70	78	$22,142 \pm 74$	$22,111 \pm 73$	$571^{+56}_{-43}$	$641^{+63}_{-49}$
	46	44	46	$22,176 \pm 89$	$22,166 \pm 79$	$539^{+69}_{-50}$	$536^{+69}_{-50}$
A2079 .....	113	89	89	$20,681 \pm 219$	$19,821 \pm 92$	$1922^{+163}_{-130}$	$864^{+73}_{-59}$
	59	52	56	$19,794 \pm 107$	$19,766 \pm 104$	$711^{+82}_{-61}$	$778^{+90}_{-67}$
A2089 .....	119	72	75	$21,924 \pm 101$	$22,028 \pm 89$	$793^{+76}_{-59}$	$770^{+74}_{-58}$
	46	36	39	$22,026 \pm 94$	$22,042 \pm 95$	$515^{+75}_{-52}$	$591^{+86}_{-60}$
A2107 .....	75	68	68	$12,336 \pm 86$	$12,338 \pm 82$	$674^{+67}_{-52}$	$675^{+67}_{-52}$
	75	68	68	$12,336 \pm 86$	$12,338 \pm 82$	$674^{+67}_{-52}$	$675^{+67}_{-52}$
A2124 .....	64	63	63	$19,674 \pm 116$	$19,664 \pm 107$	$847^{+88}_{-67}$	$851^{+88}_{-68}$
	62	61	61	$19,689 \pm 119$	$19,684 \pm 110$	$858^{+91}_{-69}$	$862^{+91}_{-69}$
A2199 .....	145	137	139	$9,039 \pm 69$	$9,017 \pm 70$	$780^{+52}_{-44}$	$826^{+55}_{-46}$
	133	127	127	$8,986 \pm 71$	$8,948 \pm 71$	$775^{+54}_{-45}$	$796^{+55}_{-46}$
A2634 .....	176	125	126	$9,409 \pm 82$	$9,378 \pm 78$	$878^{+62}_{-51}$	$878^{+62}_{-51}$
	137	114	115	$9,466 \pm 84$	$9,424 \pm 81$	$865^{+64}_{-53}$	$864^{+64}_{-53}$
A2666 .....	67	49	50	$8,042 \pm 89$	$8,131 \pm 81$	$593^{+71}_{-53}$	$574^{+69}_{-51}$
	54	34	37	$8,263 \pm 56$	$8,236 \pm 58$	$307^{+47}_{-33}$	$353^{+53}_{-37}$
A2670 .....	285	224	236	$22,840 \pm 67$	$22,830 \pm 67$	$916^{+47}_{-41}$	$1035^{+53}_{-46}$
	226	191	196	$22,816 \pm 79$	$22,860 \pm 76$	$1007^{+56}_{-48}$	$1062^{+59}_{-51}$

NOTE.—For each cluster, the first line gives the cluster properties based on known redshifts within  $3.5 h_{75}^{-1}$  Mpc of the brightest cluster galaxy, and the second line represents the same cluster with the radius restricted to  $1.5 h_{75}^{-1}$  Mpc. Col. (1): cluster name; col. (2): total number of redshifts,  $N_{\text{obs}}$ , in the sample for that cluster—in some cases, identifiable background clusters have been removed; col. (3): number of cluster members,  $N_{\text{cl}}$ , remaining after  $3 \sigma$  clipping; col. (4): number of redshifts,  $N_{\text{bi}}$ , used in the biweight calculations—these are required to be within  $6000 \text{ km s}^{-1}$  of the brightest cluster galaxy; col. (5): observed mean cluster velocity,  $\bar{v} = cz$ , after  $3 \sigma$  clipping and estimated error in the mean cluster velocity in kilometers per second; col. (6): biweight estimate of the observed location,  $C_{\text{bi}}$ , and estimated error in the location in kilometers per second; col. (7): velocity dispersion,  $\sigma$ , corrected for measurement error after  $3 \sigma$  clipping of galaxy membership and estimated error in the velocity dispersion, in kilometers per second; col. (8): biweight estimate of the scale,  $S_{\text{bi}}$ , corrected for measurement error and cosmological expansion, and estimated error in  $S_{\text{bi}}$  in kilometers per second.

If clusters are formed through the hierarchical merging of smaller clusters, then cDs would be formed in one of these merging subclusters. We could then hope to detect the residual motion of the cD with respect to the merging clusters. Malumuth (1992) has explored with simulations whether it is possible to form cD galaxies with significant peculiar velocities in rich clusters via dynamical friction. He found that after  $\sim 10^{10}$  yr, the cD galaxies in his simulated clusters had a distribution of peculiar velocities that was significantly different than the observed clusters. The efficiency of dynamical friction and two-body relaxation over that timescale resulted in the cD being dragged to the bottom of the potential well with little peculiar velocity. He concluded that his models could be reconciled with observations only if (1) clusters that form cD galaxies are relatively young, (2) cD galaxies are a relatively recent phenomenon, (3) clusters are not entirely virialized, (4) cD galaxies are not formed in their present environment but have been added from elsewhere, or (5) dynamical friction in the real universe is not as efficient as in the simulations.

The observational data employed by Malumuth (1992) for comparison with his models were culled from many different sources in the literature, which used different data reduction and analysis techniques and was not an objective sample of clusters. Having established that at least some cD galaxies have significant peculiar velocities, Hill & Oegerle (1993, hereafter Paper I) began a systematic survey to determine the accurate peculiar velocities of cD galaxies in a statistically complete sample of clusters. This survey also included extensive dynamical study of the host clusters. The object of the survey was to determine whether the known peculiar velocities of cDs represent the statistical tail of a distribution of velocities in which the cD galaxy is at rest in the cluster potential or whether the peculiar velocities were telling us something important about the process of cD and cluster formation. This paper represents the conclusion of that systematic survey.

The questions that we attempt to answer here are whether cD galaxies in rich clusters have significant peculiar velocities relative to the cluster potential well and whether the number and distribution of those peculiar velocities are able to constrain the models of cD formation and growth.

In § 2 we review the selection and subsequent expansion of the cluster sample for this study. In § 3 we provide a detailed dynamical analysis of the 11 clusters that were observed by Hill & Oegerle (1998, hereafter Paper III) In § 4 we discuss the observed cD peculiar velocities and the effects of substructure in the clusters. In § 5, we briefly review the formation scenarios for cD galaxies. Finally in § 6 we report the conclusions of this study.

## 2. CLUSTER SAMPLE

To arrive at a tractable sample of clusters, we started with the Hoessel, Gunn, & Thuan (1980, hereafter HGT) Abell cluster sample (Paper I). HGT selected their sample of brightest cluster galaxies from all northern Abell clusters with (1) absolute values of galactic latitude larger than  $30^\circ$ , (2) richness class  $\geq 1$  and distance class  $\leq 4$ , and (3) richness class 0 and distance class  $\leq 3$ . We have further narrowed the HGT sample using the following additional constraints: the cluster must (1) be of Rood-Sastry type cD as defined by Struble & Rood (1987), (2) have redshift less than 0.08, and (3) have declination  $-11^\circ < \delta < +72^\circ$ . All our obser-

vations were obtained on Kitt Peak in Arizona, hence the lower declination cutoff at  $-11^\circ$ . The upper declination cutoff of  $+72^\circ$  was due to a telescope limit when observing with the MX multifiber spectrometer.

During the course of this study we discovered that cluster A1927 actually had a mean redshift of 0.0948, placing it outside our original sample constraints. To retain A1927 in our sample and keep the sample complete, we have expanded the redshift limit to 0.095 and included A1651 in the sample. The resulting sample of 25 Abell clusters is listed in Table 1.

Data sets of suitable size and quality for use in this study now exist in the literature for some of the clusters in our sample. Redshifts for A2670 have been published by Sharples et al. (1988). Redshift data for A85 and A2052 have been published by Malumuth et al. (1992). As part of our program, we have previously published data for A2107 (Oegerle & Hill 1992) and A2634 (Pinkney et al. 1993). In Paper I, we presented redshifts for A193, A399, A401, A1795, A1809, A2063, and A2124. Redshifts for A2029 were presented by Oegerle, Hill, & Fitchett (1995) as part of another study. In Paper III we presented redshift data for A779, A1691, A1749, A1767, A1837, A1927, A2067, A2079, A2089, A2199 and A2666.

Throughout this paper we have used  $q_0 = \frac{1}{2}$ , and parameterized the Hubble constant by using the term  $h_{75}$ , where  $H_0 = 75 h_{75} \text{ km s}^{-1} \text{ Mpc}^{-1}$ .

## 3. KINEMATICS OF THE 11 NEWLY OBSERVED CLUSTERS

In this section, we present an analysis of the 11 galaxy clusters for which redshift data were published in Paper III, complementing previous analyses of the other clusters in our sample published previously (and cited above). First we discuss the velocity distributions and dispersions of these clusters and then investigate evidence for substructure. This is followed by notes on individual clusters that warrant further discussion.

### 3.1. Velocity Distributions

We have supplemented our observations with additional velocities from the literature within a radius of approximately  $3.5 h_{75}^{-1}$  Mpc. In general when adding velocities from the literature we have tried to be complete through mid-1998. It should be noted, however, that not all clusters have redshift data out to a radius as large as  $3.5 h_{75}^{-1}$  Mpc.

To determine cluster membership, we have employed the “3  $\sigma$  clipping” technique of Yahil & Vidal (1977), with a slight variation. All computations are made not on the *observed* heliocentric-corrected velocities but on their cosmologically corrected values:  $v = c[(1+z)^2 - 1] / [(1+z)^2 + 1]$ . Initially, we exclude from the distribution any galaxy more than  $6000 \text{ km s}^{-1}$  from the velocity of the BCG. We chose to cut around the velocity of the BCG rather than the median velocity of all galaxies in the sample to minimize the effects of background groups and clusters and the surrounding supercluster environment. After making this cut, we then proceed with the 3  $\sigma$  clipping as described by Yahil & Vidal (1977). The mean velocity and dispersion are computed from the remaining galaxies, and then the galaxy furthest from the mean is clipped from the distribution if it is more than 3  $\sigma$  distant. The mean and dispersion are recomputed after each galaxy is clipped. This procedure is followed until the furthest outlying galaxy is accepted as a cluster member, at which point the clipping

procedure is halted. Determination of membership is usually straightforward for most clusters in our sample, with several notable exceptions that are discussed below. In addition to computing the mean and standard deviation (dispersion) of the cluster members, we have also computed the more robust quantities,  $C_{\text{bi}}$  and  $S_{\text{bi}}$ , which are biweight measures of location and scale as described by Beers, Flynn, & Gebhardt (1990). When computing these values, the  $3\sigma$  clipping technique is not used at all. Instead, these robust quantities are computed from all galaxy velocities within  $\pm 6000 \text{ km s}^{-1}$  of the velocity of the BCG.

The histograms of observed velocities for the 11 clusters are shown in Figure 1. In the figures, the arrow marks the observed velocity of the cD galaxy and the dashed line is a normalized Gaussian, centered at  $C_{\text{bi}}$ , with a dispersion equal to  $\sigma = (1+z)S_{\text{bi}}$  computed from all galaxies within  $3.5 h_{75}^{-1} \text{ Mpc}$ . The Gaussian extends to  $\pm 3\sigma$  in velocity. All galaxy velocities within  $\pm 6000 \text{ km s}^{-1}$  from  $C_{\text{bi}}$  are plotted in Figure 1, not just the cluster members.

The mean observed cluster velocities (heliocentric  $cz$  in kilometers per second), velocity dispersions corrected for measurement error, and values of biweight location,  $C_{\text{bi}}$ , and scale,  $S_{\text{bi}}$ , are given in Table 1 for these 11 clusters plus the other 14 clusters in the sample. The velocity data for all the clusters have been reanalyzed according to the cluster membership criteria discussed above. Thus the results in Table 1 may differ from those previously reported in the literature because of small algorithmic differences or because of additional redshifts that have been measured since the original analysis. The first line for each cluster listed in Table 1 is computed for all known redshifts within  $3.5 h_{75}^{-1} \text{ Mpc}$  of the BCG. Since not all clusters have measured redshifts extending out as far as  $3.5 h_{75}^{-1} \text{ Mpc}$ , we have added a second line in Table 1, computed for all known redshifts within  $1.5 h_{75}^{-1} \text{ Mpc}$ . In cases in which the cluster is part of a larger supercluster environment or if subclustering exists at large radii, the result based on galaxies within  $1.5 h_{75}^{-1} \text{ Mpc}$  possibly provides a more meaningful picture of the true dynamical state of the cluster, at least with respect to any peculiar velocity of the cD.

### 3.2. Substructure

To investigate the shape of the cluster velocity distributions, we have calculated the  $I$  statistic, which is a sensitive indicator of non-Gaussian distributions (Teague, Carter, & Gray 1990). A distribution is considered non-Gaussian if  $I > I_{0.90}$ , where  $I_{0.90}$  is the critical value for rejecting the Gaussian hypothesis at the 90% confidence level. The values of  $I$  and  $I_{0.90}$  are given in Table 2, where we have once again presented results for two cutoffs in the outer radius of the cluster. With an outer radius of  $1.5 h_{75}^{-1} \text{ Mpc}$ , all clusters pass the Gaussian test except A1749 and A1927. A1749 has a tail to the velocity distribution extending to larger velocities. A1927 is interesting in that the distribution of galaxies within  $3.5 h_{75}^{-1} \text{ Mpc}$  is Gaussian but not if the radius is restricted to  $1.5 \text{ Mpc}$ . This will be discussed further below. A2079 and A2089 appear non-Gaussian when including galaxies from a larger radius, but this is due to their location within the Corona Borealis supercluster. Cluster velocity dispersions do change as a function of cluster radius as illustrated by the detailed analysis of A2063 by Krempc-Krygier & Krygier (1999).

We have employed the Dressler-Shectman  $\Delta$  test (Dressler & Shectman 1988) as an additional means of

TABLE 2  
NORMALITY AND SUBCLUSTERING STATISTICS

Cluster (1)	$I$ (2)	$I_{90}$ (3)	$\Delta_{\text{obs}}$ (4)	$f(\Delta_{\text{sim}} > \Delta_{\text{obs}})$ (5)	Notes (6)
A85 .....	0.89	1.04	166	0.039	Gaussian
	0.88	1.05	137	0.062	Gaussian
A193 ....	0.82	1.07	70	0.576	Gaussian
	0.82	1.07	72	0.413	Gaussian
A399 ....	0.93	1.06	85	0.549	Gaussian
	0.94	1.07	67	0.623	Gaussian
A401 ....	0.99	1.04	134	0.255	Gaussian
	0.97	1.05	97	0.406	Gaussian
A779 ....	9.29	1.06	181	0.000	Non-Gaussian
	0.56	1.09	42	0.864	Gaussian
A1651...	0.75	1.12	21	0.967	Gaussian
	0.84	1.14	20	0.862	Gaussian
A1691...	0.96	1.07	68	0.619	Gaussian
	1.00	1.08	52	0.776	Gaussian
A1749...	1.79	1.09	81	0.011	Non-Gaussian
	1.79	1.09	81	0.011	Non-Gaussian
A1767...	1.07	1.08	50	0.802	Gaussian
	1.06	1.08	46	0.868	Gaussian
A1795...	0.76	1.05	148	0.001	Gaussian
	0.74	1.06	136	0.000	Gaussian
A1809...	0.91	1.09	57	0.282	Gaussian
	0.99	1.10	50	0.219	Gaussian
A1837...	0.44	1.14	28	0.419	Gaussian
	0.65	1.15	24	0.540	Gaussian
A1927...	0.55	1.10	75	0.005	Gaussian
	2.45	1.13	55	0.040	Non-Gaussian
A2029...	0.95	1.06	99	0.164	Gaussian
	0.94	1.06	95	0.135	Gaussian
A2052...	0.92	1.07	74	0.594	Gaussian
	0.94	1.08	58	0.486	Gaussian
A2063...	0.93	1.06	71	0.679	Gaussian
	0.96	1.08	54	0.721	Gaussian
A2067...	0.80	1.07	94	0.057	Gaussian
	1.03	1.11	52	0.197	Gaussian
A2079...	5.44	1.06	181	0.000	Non-Gaussian
	0.83	1.09	34	0.974	Gaussian
A2089...	1.07	1.07	94	0.084	Non-Gaussian
	0.75	1.13	25	0.904	Gaussian
A2107...	1.00	1.07	111	0.000	Gaussian
	1.00	1.07	111	0.000	Gaussian
A2124...	0.99	1.08	67	0.318	Gaussian
	0.99	1.08	64	0.306	Gaussian
A2199...	0.90	1.04	176	0.020	Gaussian
	0.95	1.04	151	0.075	Gaussian
A2634...	1.01	1.04	165	0.044	Gaussian
	1.02	1.05	150	0.048	Gaussian
A2666...	1.07	1.10	71	0.030	Gaussian
	0.78	1.13	45	0.057	Gaussian
A2670...	0.78	1.02	308	0.004	Gaussian
	0.90	1.03	261	0.002	Gaussian

NOTE.—For each cluster, the first line gives the cluster properties based on known redshifts within  $3.5 h_{75}^{-1} \text{ Mpc}$  of the brightest cluster galaxy, and the second line represents the same cluster with the radius restricted to  $1.5 h_{75}^{-1} \text{ Mpc}$ . Col. (1): cluster name; col. (2):  $I$  statistic; col. (3):  $I_{90}$  threshold for the  $I$  statistic to indicate a non-Gaussian distribution; col. (4): observed Dressler-Shectman  $\Delta$  statistic; col. (5): fraction,  $f$ , of shuffled clusters that have Dressler-Shectman  $\Delta$  greater than that of the observed cluster.

searching for the presence of substructure in velocity and/or dispersion. For each cluster member the term  $\delta_n^2 = 11[(\bar{v}_{10c} - \bar{v}_{cl})^2 + (\sigma_{10c} - \sigma_{cl})^2]/\sigma_{cl}^2$  is calculated, where  $\bar{v}_{10c}$  and  $\sigma_{10c}$  are the mean velocity and dispersion for the 10 nearest neighbor galaxies and  $\bar{v}_{cl}$  and  $\sigma_{cl}$  are the global cluster

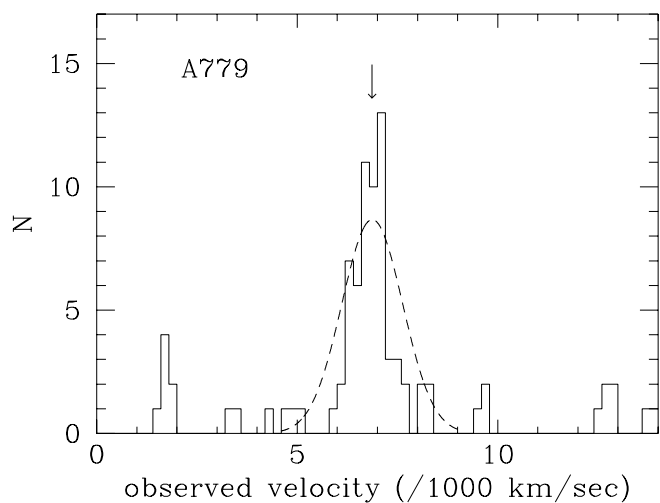


FIG. 1a

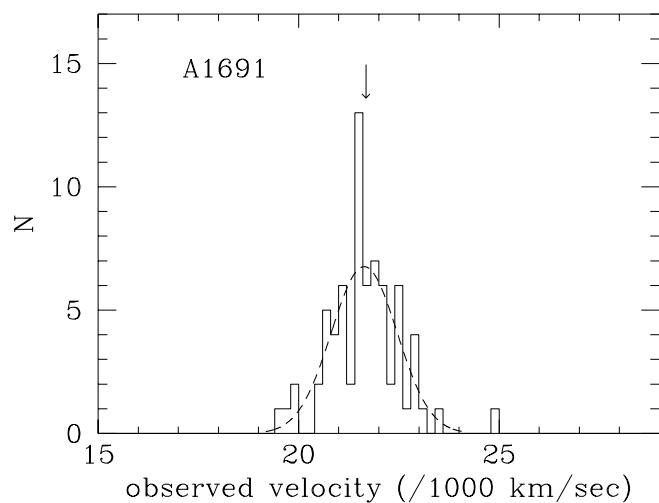


FIG. 1b

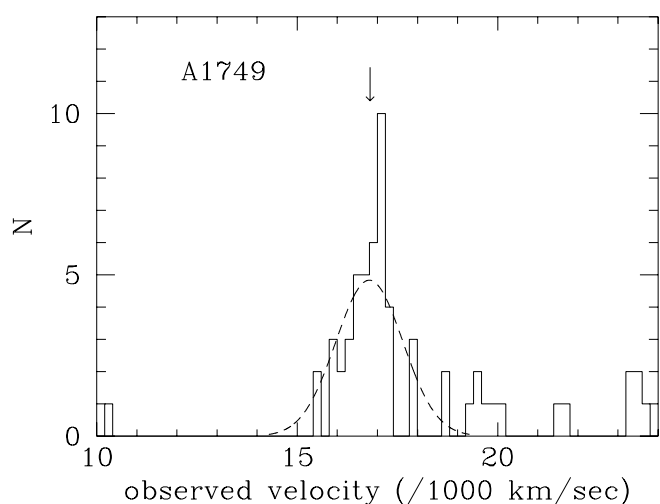


FIG. 1c

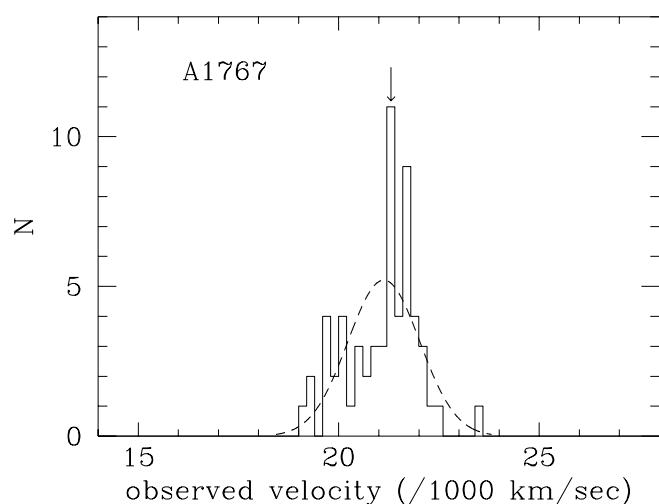


FIG. 1d

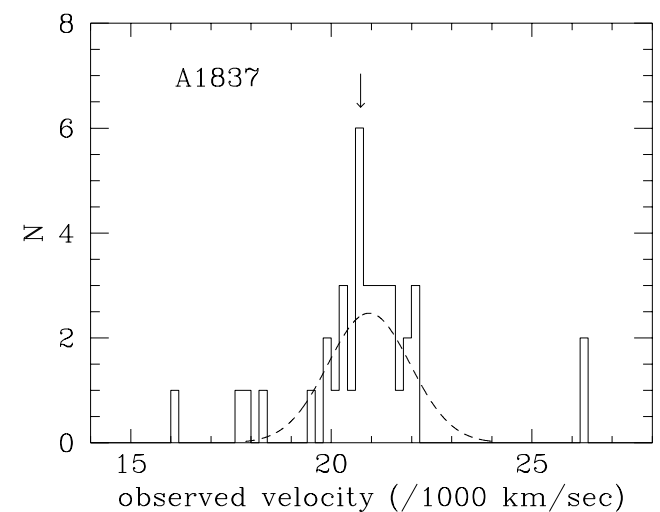


FIG. 1e

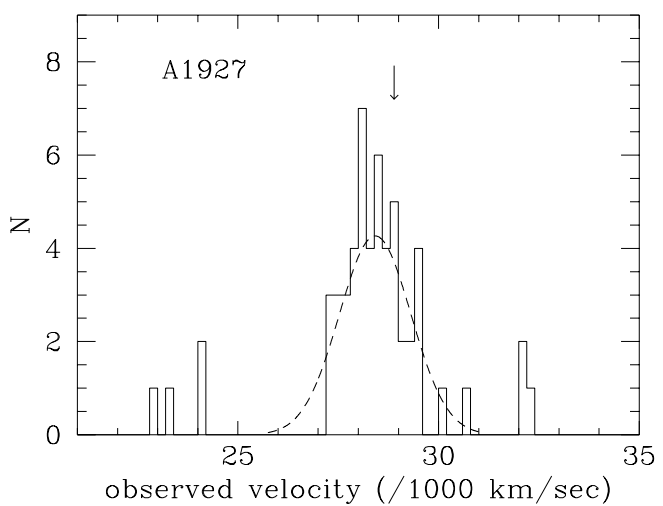


FIG. 1f

FIG. 1.—Histograms of observed velocities for 11 Abell clusters. The velocity bin size is  $200 \text{ km s}^{-1}$ . The arrow marks the velocity of the cD. The data for A2067 include the velocities in the nearby cluster A2061. The dashed line is a Gaussian centered at the biweight location,  $C_{\text{bi}}$ , with  $\sigma = (1+z)S_{\text{bi}}$ , where  $S_{\text{bi}}$  is the robust biweight scale (dispersion) of the cluster.  $C_{\text{bi}}$  and  $S_{\text{bi}}$  are computed from galaxies within  $3.5 h^{-1}_{75} \text{ Mpc}$  of the cluster center. The dashed line extends to  $\pm 3 \sigma$ . Plots are shown for clusters (a) A779, (b) A1691, (c) A1749, (d) A1767, (e) A1837, (f) A1927, (g) A2067/A2061, (h) A2079, (i) A2089, (j) A2199, and (k) A2666.

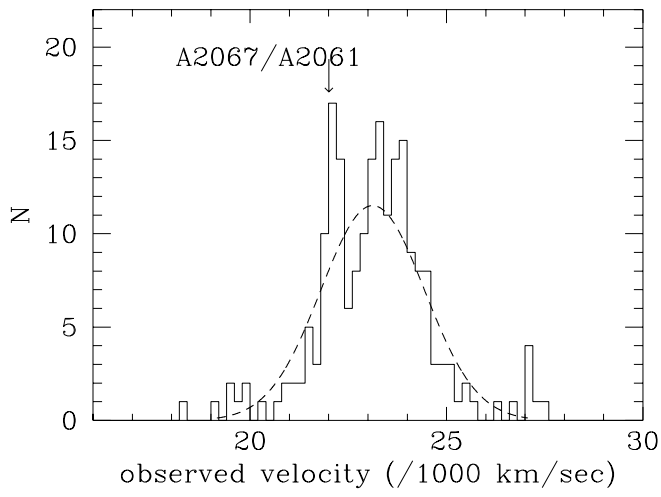


FIG. 1g

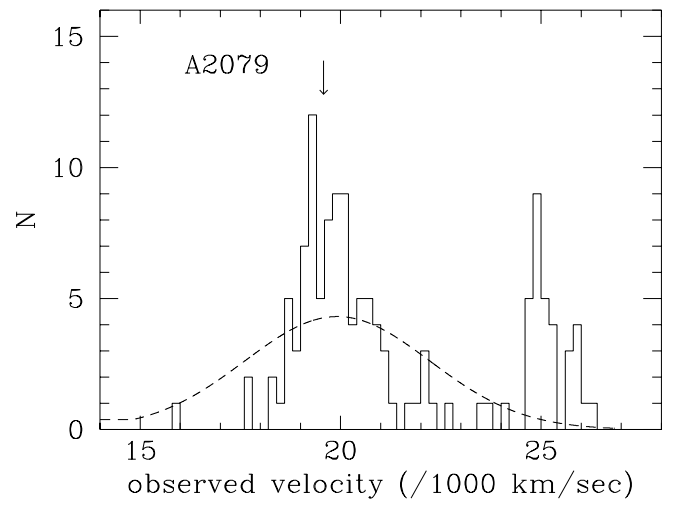


FIG. 1h

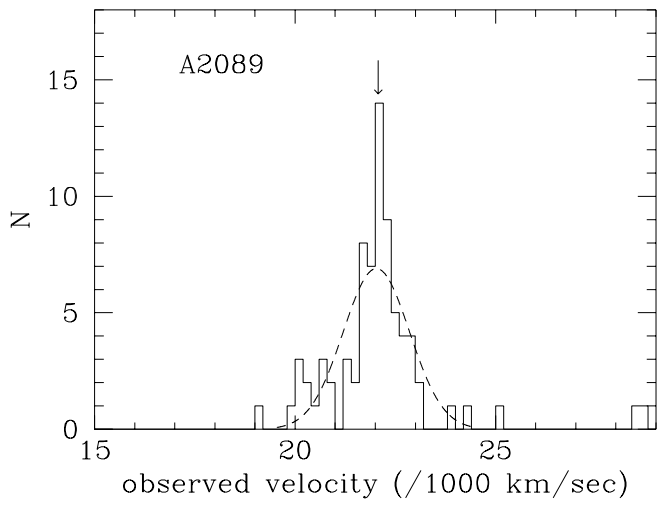


FIG. 1i

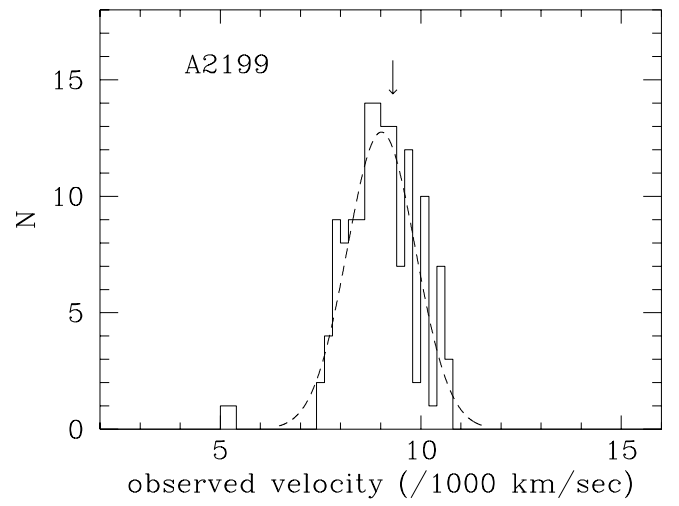


FIG. 1j

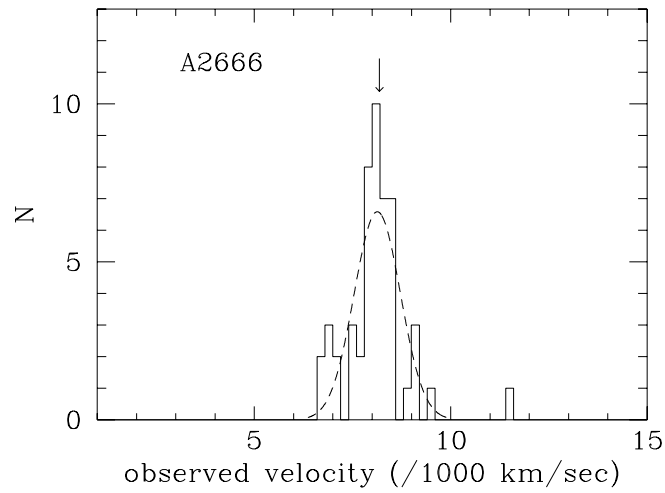


FIG. 1k

values. For each cluster, we have plotted circles at the position of each galaxy in Figure 2, where the diameter of the circle is proportional to  $e^\delta$ . A large circle (i.e., large value of  $\delta$ ) indicates a galaxy that is deviant in either velocity or dispersion compared with nearby galaxies (projected on the sky). A single large circle does not indicate anything statistically significant, but groups of large circles do indicate the presence of subclustering in velocity or dispersion. The cumulative deviation of a cluster,  $\Delta_{\text{obs}}$ , is then computed by summing  $\delta_n$  over all  $n$  observed galaxies. The statistical significance of the deviation is determined by Monte Carlo simulations in which the observed velocities are randomly assigned to galaxies at the observed galaxy locations, and  $\Delta_{\text{sim}}$  is computed for each of these simulated clusters. For each of the 11 clusters under study here, we have constructed 1000 simulated clusters and computed  $\Delta_{\text{sim}}$  for each simulation. The results are shown in Table 2, where we list  $\Delta_{\text{obs}}$  and the fraction of simulated clusters with  $\Delta_{\text{sim}} > \Delta_{\text{obs}}$ . Clusters with very small values of  $f(\Delta_{\text{sim}} > \Delta_{\text{obs}})$  contain statistically significant subclustering. For example, from Table 2, A2670 has  $f(\Delta_{\text{sim}} > \Delta_{\text{obs}}) = 0.002\text{--}0.004$ , depending on the radius of included galaxies—only 2–4 simulated clusters out of 1000 simulations had  $\Delta_{\text{sim}} > \Delta_{\text{obs}}$ . This indicates subclustering that is significant at the  $\gtrsim 3\sigma$  level.

### 3.3. A779

A779 presents a real difficulty for the  $3\sigma$  clipping technique, since there are galaxies spread over a large range of velocities. A779 is at low redshift ( $z \sim 0.023$ ) and therefore, its projected size on the sky is quite large when considering as potential members all galaxies within a radius of  $3.5 h_{75}^{-1}$  Mpc. The initial dispersion computed from the distribution is so large that effectively no galaxies are clipped (beyond the initial  $\pm 6000 \text{ km s}^{-1}$  cut). Hence, the standard velocity dispersion computed for this distribution is extremely large— $2256 \text{ km s}^{-1}$ , as reported in Table 1. The  $3\sigma$  clipping technique arrives at different results depending the somewhat arbitrary decision to limit the initial cluster galaxy sample to those galaxies within  $\pm 6000 \text{ km s}^{-1}$ . If the cut is decreased to only  $\pm 5000 \text{ km s}^{-1}$ , then the procedure successfully eliminates velocity outliers and arrives at a dispersion of  $\sigma = 489 \text{ km s}^{-1}$ ! The more robust biweight scale,  $S_{\text{bi}}$ , is  $741 \text{ km s}^{-1}$ . The Gaussian overlay in Figure 1 is drawn using this value of  $S_{\text{bi}}$ , but it still appears somewhat broader than the true velocity distribution. The value of  $S_{\text{bi}}$  computed within a radius of  $1.5 h_{75}^{-1}$  Mpc is about 30% smaller ( $512 \text{ km s}^{-1}$ , as reported in Table 1) and appears to be a better representation of the dispersion of the true cluster. A quick look at Figure 2a indicates why the computed dispersion is so large when galaxies at large radii are included. There are a number of galaxies  $\sim 5000''$  to the northeast of A779 that lie far from the central velocity of the cluster. A cutoff radius of  $1.5 h_{75}^{-1}$  Mpc at this redshift eliminates all galaxies more than  $3500''$  from the cluster center. This is why the velocity dispersion reported in Table 1 is so different depending on the choice of cutoff radius.

### 3.4. A1749

In A1749, there are six galaxies in the velocity range  $19,000\text{--}20,000 \text{ km s}^{-1}$  that survive the  $3\sigma$  clipping to provide a non-Gaussian velocity distribution in this cluster, as well as an inflated velocity dispersion. As shown in Table 1, the dispersion of these cluster members is  $1048 \text{ km s}^{-1}$ , while the more robust value of  $S_{\text{bi}}$  is  $791 \text{ km s}^{-1}$ . These

galaxies on the high-velocity tail stand out quite clearly in Figure 2c, where they appear to form a subcluster to the southeast of the center of A1749.

### 3.5. A1927

The kinematics of A1927 are quite unusual. The histogram of velocities shown in Figure 1f appears normal enough, but the spatial distribution of velocities indicates subclustering. Figure 2f (bottom) shows that a preponderance of galaxies with velocities below the cluster mean (*open and solid squares*) lie to the south and west of the cluster center, while those galaxies with velocities larger than the cluster mean (*open and solid triangles*) lie to north and east of the cluster center. This situation is similar to the spatial velocity distribution that we found for A2107 (Oegerle & Hill 1992). It is difficult to determine the true cause of this distribution; as discussed in Oegerle & Hill (1992), it could just be a coincidental alignment of subclusters about the cD or it could indicate rotation of the cluster about the cD.

### 3.6. A2067 and A2061

A2067 is a member of the Corona Borealis supercluster. Consequently, our redshift survey of A2067 includes the nearby cluster A2061, which is to the southwest of A2067. The velocity distribution shown in Figure 1 includes velocities from both clusters, resulting in its bimodal appearance. The velocity of the cD in A2067, indicated by the arrow, is  $22,005 \text{ km s}^{-1}$ , while the velocity of the BCG in A2061 (galaxy 316 in the tables of Paper III) is  $23,725 \text{ km s}^{-1}$ . The fact that A2067 and A2061 are separate clusters is also easily seen in the Dressler-Shectman diagram shown in Figure 2g (top).

Given the projected spatial separation on the sky of  $\sim 30'$  for the brightest cluster members and their  $1720 \text{ km s}^{-1}$  difference in radial velocity, it is possible to crudely separate the two clusters by a simple consideration of each galaxy's velocity and position. For each galaxy, we compute a threshold velocity,  $v_t = \bar{v} - \delta v |r_1 - r_2| / 2r_{12}$ , where  $\bar{v}$  is the average of the A2067 and A2061 BCG velocities,  $\delta v$  is the absolute value of the difference in velocities of the BCGs,  $r_1$  is the distance of the galaxy to the cD in A2067,  $r_2$  is the distance of the galaxy to the A2061 BCG, and  $r_{12}$  is the distance between the BCGs. If the velocity of the galaxy in question is greater than  $v_t$ , then that galaxy is assigned to A2061; otherwise it is assigned to A2067. This probabilistic separation technique is not by any means unique, but it is certainly more representative of the distributions of the individual clusters. The velocity histograms for the resulting members assigned to A2067 and A2061 are shown in Figure 3. The results quoted in Table 1 are for A2067 only as determined from our separation; 200 velocities from Small, Sargeant, & Hamilton (1997) have been included in this analysis of the clusters A2067 and A2061. Small et al. (1998) discuss the structure and dynamics of the larger supercluster.

Dynamical results for A2061 are not reported in Table 1, since this cluster is not a member of our cD sample, but will be reported here. Based on 126 observed velocities (after separating out those belonging to A2067), the number of probable cluster members surviving the  $3\sigma$  clipping is 118. We find a mean observed velocity of  $23,721 \pm 67 \text{ km s}^{-1}$  and a biweight location of  $C_{\text{bi}} = 23,699 \pm 70 \text{ km s}^{-1}$ . The standard velocity dispersion is  $673^{+49}_{-40} \text{ km s}^{-1}$ , and the biweight scale is  $780^{+57}_{-47} \text{ km s}^{-1}$ .

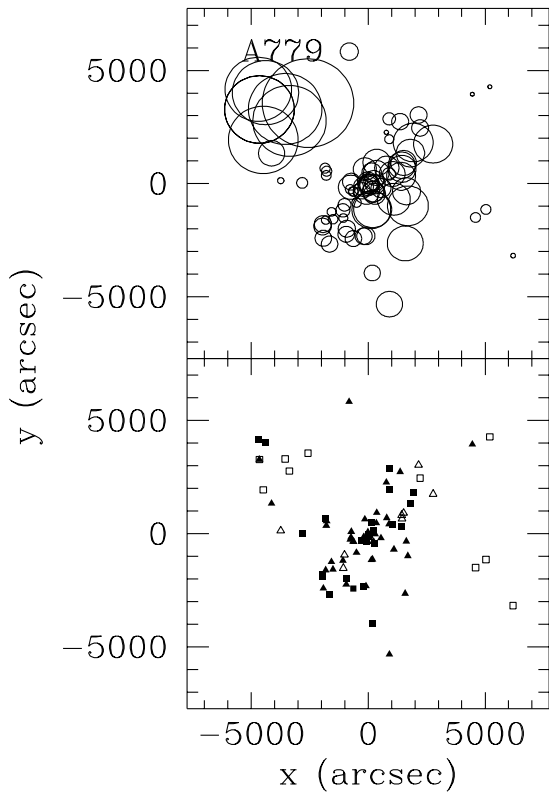


FIG. 2a

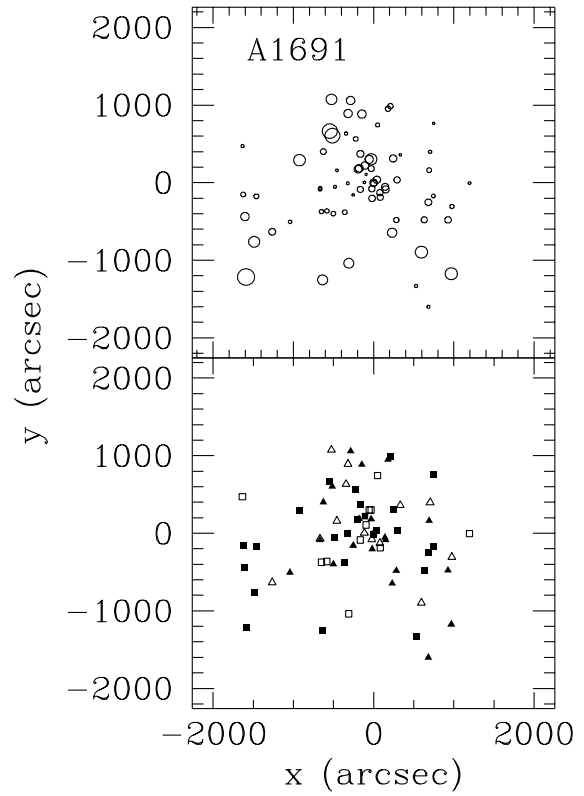


FIG. 2b

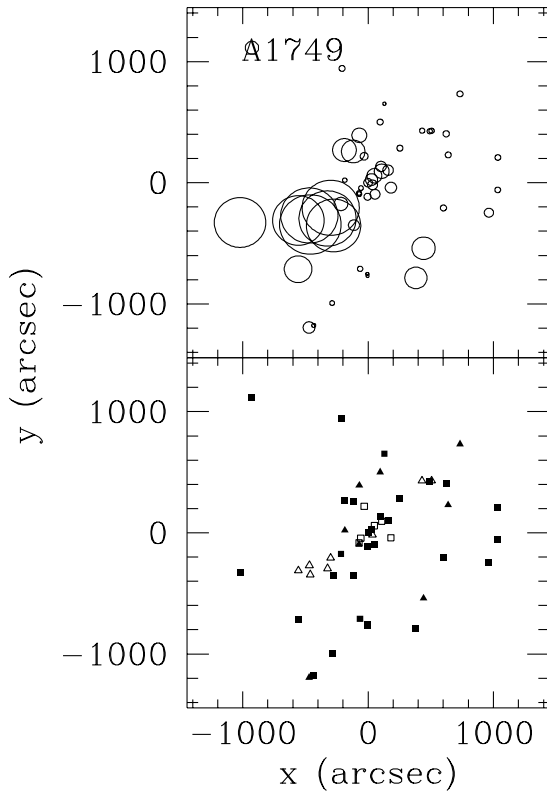


FIG. 2c

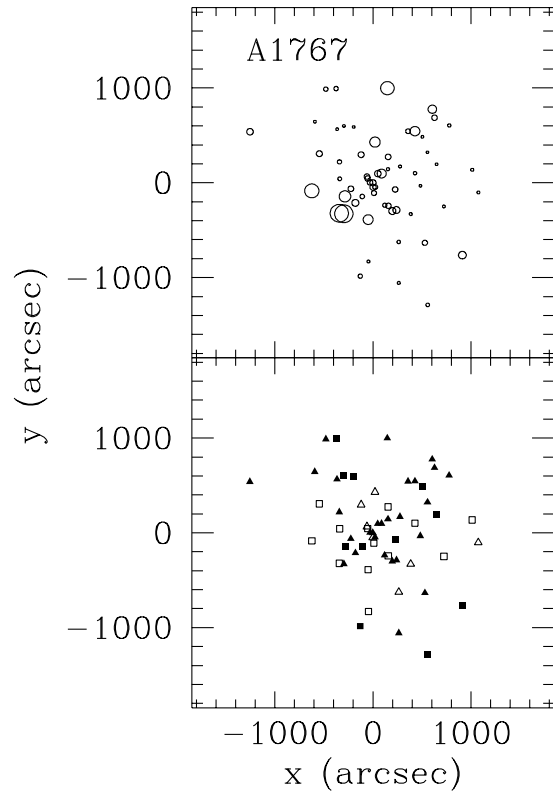


FIG. 2d

FIG. 2.—*Top*: Cluster member galaxies plotted as open circles, where the diameter of the circle is proportional to  $e^{\delta}$ , from the Dressler-Shectman test; *bottom*, same cluster members plotted with symbols coded according to where they lie in the cluster velocity distribution. Galaxies with velocities  $\bar{v} - 3\sigma_r \leq v_{\text{obs}} < \bar{v} - \sigma_r$  are plotted as open squares, those with  $\bar{v} - \sigma_r \leq v_{\text{obs}} < \bar{v}$  are plotted as filled squares, those with  $\bar{v} \leq v_{\text{obs}} < \bar{v} + \sigma_r$  as filled triangles, and those with  $\bar{v} + \sigma_r \leq v_{\text{obs}} \leq \bar{v} + 3\sigma_r$  as open triangles. The cD galaxy is plotted at  $(x, y) = (0, 0)$ , with north at the top of the plot and east to the left. Plots are shown for clusters (a) A779, (b) A1691, (c) A1749, (d) A1767, (e) A1837, (f) A1927, (g) A2067/A2061, (h) A2079, (i) A2089, (j) A2199, and (k) A2666.

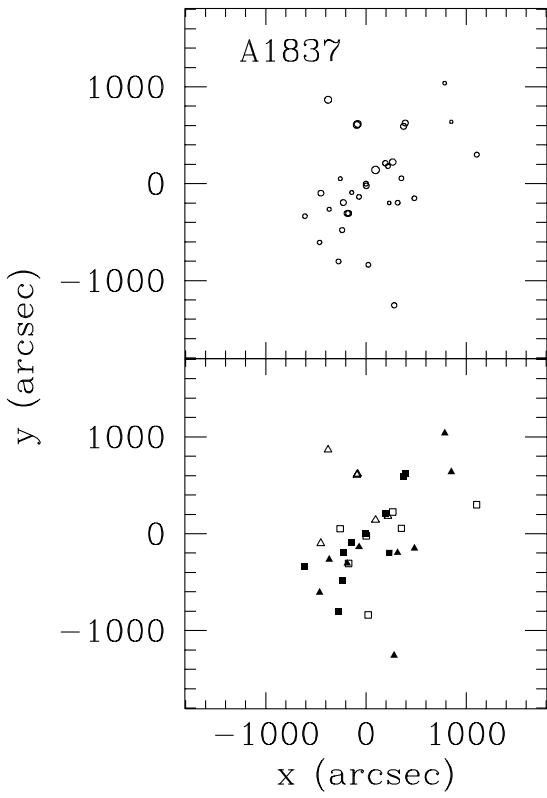


FIG. 2e

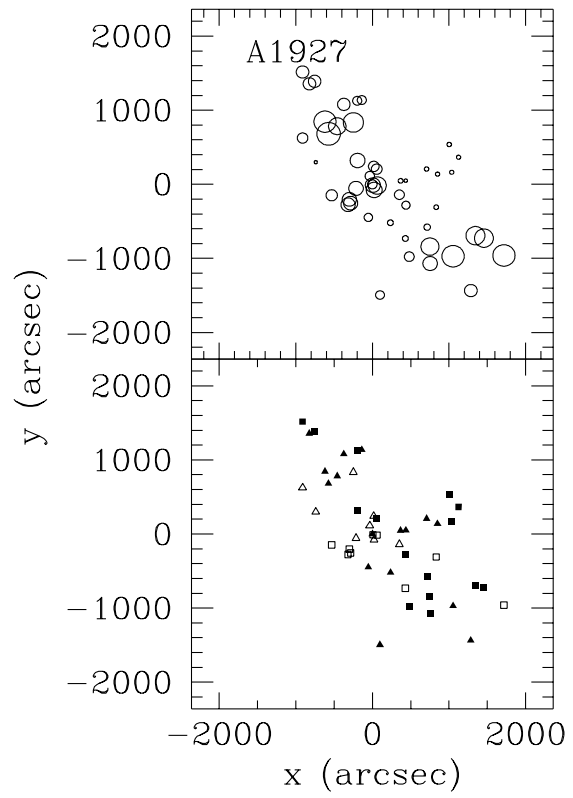


FIG. 2f

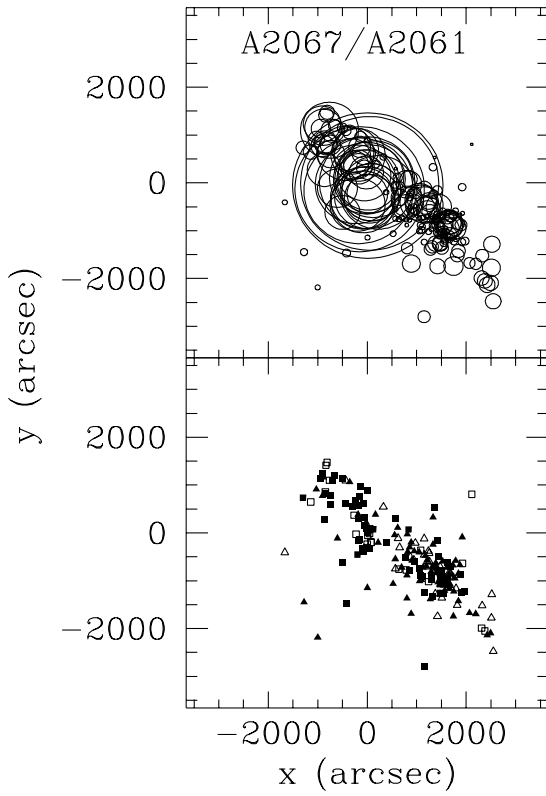


FIG. 2g

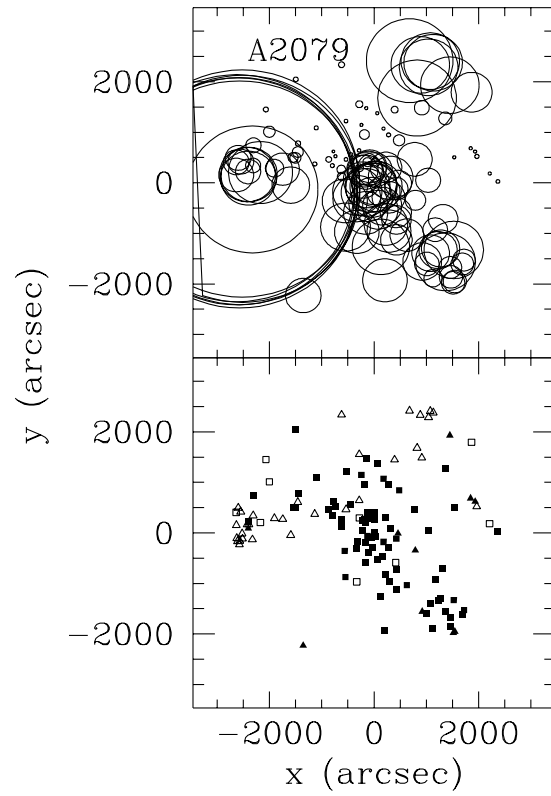


FIG. 2h

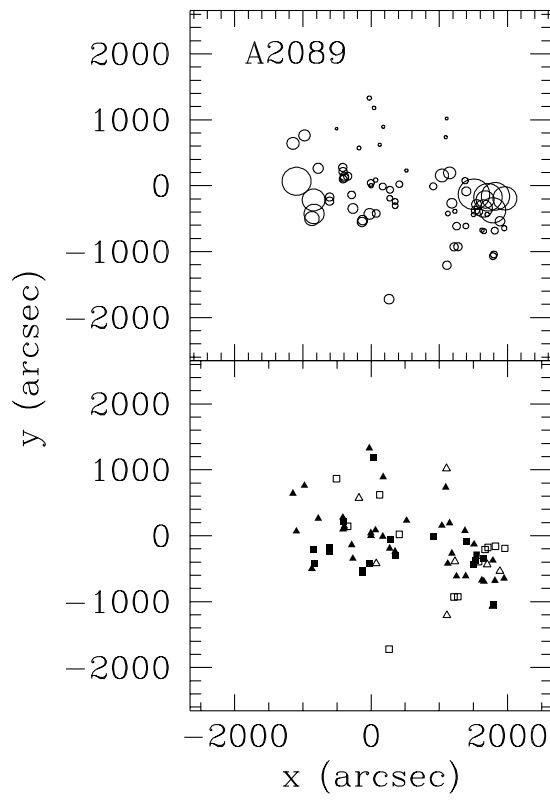


FIG. 2i

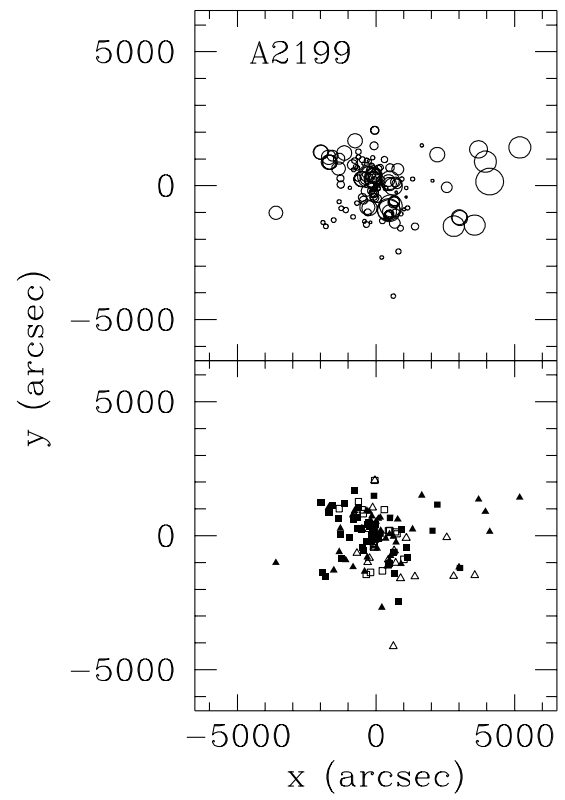


FIG. 2j

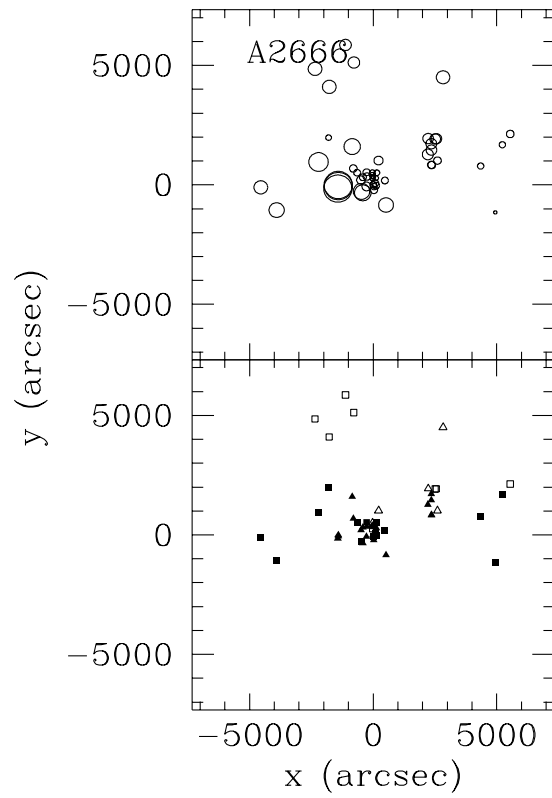


FIG. 2k

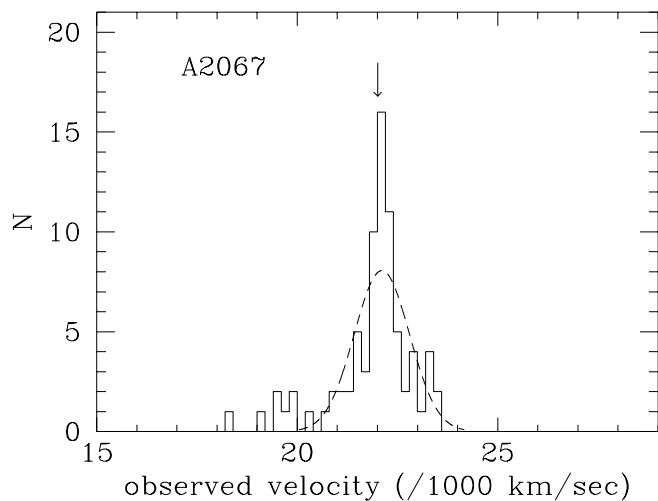


FIG. 3a

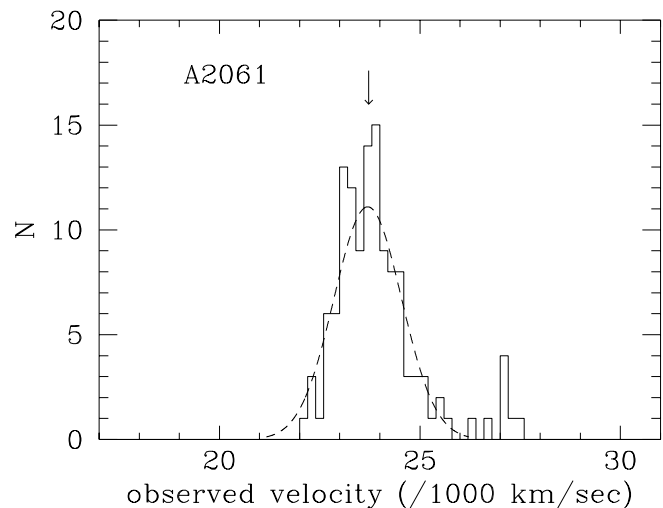


FIG. 3b

FIG. 3.—Histograms of observed velocities in A2067 and A2061 after separating the two clusters, based on galaxy velocities and positions. The bin size is  $200 \text{ km s}^{-1}$ . After the cluster separation, the velocities of the brightest cluster galaxies in both A2067 and A2061 are close to their respective mean cluster velocities.

### 3.7. A2079

A2079 is also a member of the Corona Borealis supercluster. The cluster analysis is complicated by several groups of galaxies near  $25,000 \text{ km s}^{-1}$ . These groups of high-velocity galaxies are evident in the Dressler-Shectman diagram in Figure 2h. These groups are located  $\sim 2500''$  to the east and northwest of the cluster center. These galaxies are not easily rejected by  $3\sigma$  clipping or by the biweight estimators. Therefore we report velocity and dispersion results in Tables 1, 2, and 3 based on a restricted radius of  $2200''$  ( $2.77 h_{75}^{-1} \text{ Mpc}$ ) around the BCG. The galaxies outside this radius are shown in Figures 1h and 2h. The overplotted Gaussian in Figure 1h represents the result from all the velocities, not the dispersion from the restricted radius. After exclusion of these outlying galaxies, the velocity distribution in A2079 passes the  $I$  statistic test for Gaussianity, and the Dressler-Shectman test indicates no further evidence for subclustering.

### 3.8. A2089

A2089 is also part of the Corona Borealis supercluster, however it does not have severe problems with overlapping clusters or groups. Our analysis includes 50 redshifts from Small et al. (1997), although many of them are background galaxies. A spatially distinct group of galaxies lies  $\sim 1700''$  to the west of the A2089 cD galaxy. When these galaxies are included in the cluster, the velocity distribution is non-Gaussian and the Dressler-Shectman test indicates that the subclustering is significant at the  $2\sigma$  level (i.e., only  $\sim 8\%$  of the simulated clusters had  $\Delta_{\text{sim}} > \Delta_{\text{obs}}$ ). With a radius cutoff of  $1.5 h_{75}^{-1} \text{ Mpc}$ , the cluster galaxies have a Gaussian velocity distribution with no subclustering.

### 3.9. A2199

A2197 is a neighboring cluster to A2199, and has roughly the same redshift. However, the vast majority of the galaxies observed by us are easily identified as belonging to A2199. We have excluded from the A2199 analysis those galaxies that lie north of declination  $+40^{\circ}25'$ , defined as the boundary between A2197 and A2199 by Gregory & Thompson

(1984). The cluster passes the  $I$  statistic test for having a Gaussian velocity distribution, although the Dressler-Shectman statistic indicates subclustering at a marginally significant ( $\sim 2\sigma$ ) level. Recent X-ray images of A2199 have shown that the hot X-ray-emitting gas, which presumably follows the shape of the gravitational potential, is elongated (Siddiqui, Stewart, & Johnstone 1998). In addition, a study of this cluster in the radio and X-ray by Owen & Eilek (1998) indicates that the core of A2199 is complex, and a simple, spherical cooling flow model cannot reproduce the observed data.

### 3.10. A2666

A2666 is located in the background of the Perseus-Pisces supercluster, along with A2634 and A2622. Scodreggio et al. (1995) provide a detailed study of the supercluster environment. Here we concentrate on A2666 itself. The field includes galaxies at the velocity of A2622 even though that cluster is  $3^{\circ}$  to the west. This is a very poor cluster (Abell richness class 0), and the galaxies within  $1.5 h_{75}^{-1} \text{ Mpc}$  have a very small velocity dispersion ( $307 \text{ km s}^{-1}$  as reported in Table 1). This dispersion is inflated to  $593 \text{ km s}^{-1}$  when considering a larger field of view, presumably because of the inclusion of galaxies affected by the supercluster kinematics.

## 4. PECULIAR VELOCITIES OF cD GALAXIES

One of the principal goals of this survey is to determine the nature and frequency of peculiar velocities of cD galaxies. We define cD peculiar velocity as  $v_p = v_{\text{cD}} - v_{\text{cl}}$ , where  $v_{\text{cl}}$  is the mean velocity of the cluster, with all velocities cosmologically corrected. Peculiar velocities for all the clusters in the sample are reported in Table 3. We have also tabulated the “robust” peculiar velocity,  $v_{\text{pr}} = v_{\text{cD}} - C_{\text{bi}}$ , which employs the biweight location instead of the mean cluster velocity. The significance of these peculiar velocities depends on both the uncertainty in the velocity of the cD galaxy,  $\epsilon_{\text{cD}}$ , and the uncertainty in the mean velocity or biweight location,  $\epsilon_{\text{cl}}$ , of the cluster potential well. The uncertainty in the latter quantity is a function of the cluster velocity dispersion and the number of measured galaxies.

TABLE 3  
cD PECULIAR VELOCITIES

Cluster (1)	$v_p$ (2)	$v_{pr}$ (3)	$S$ (4)	$S_r$ (5)
A85 .....	131 ± 100	62 ± 103	1.31	0.60
	151 ± 112	79 ± 117	1.34	0.67
A193 ....	-93 ± 102	-119 ± 109	0.91	1.09
	-93 ± 102	-117 ± 109	0.91	1.07
A399 ....	-134 ± 126	-143 ± 131	1.06	1.09
	-51 ± 141	-36 ± 144	0.36	0.25
A401 ....	179 ± 114	209 ± 115	1.57	1.81
	166 ± 131	203 ± 134	1.26	1.51
A779 ....	132 ± 249	-3 ± 75	0.53	0.04
	55 ± 55	23 ± 67	1.00	0.34
A1651 ...	219 ± 167	252 ± 186	1.31	1.35
	234 ± 178	258 ± 192	1.31	1.34
A1691 ...	61 ± 91	39 ± 92	0.67	0.42
	10 ± 90	-7 ± 87	0.11	0.08
A1749 ...	-332 ± 147	16 ± 106	2.25	0.15
	-332 ± 147	16 ± 106	2.25	0.15
A1767 ...	214 ± 114	167 ± 114	1.87	1.46
	213 ± 118	164 ± 117	1.80	1.39
A1795 ...	228 ± 83	188 ± 93	2.73	2.01
	235 ± 88	187 ± 100	2.66	1.87
A1809 ...	-80 ± 100	-63 ± 105	0.80	0.60
	-113 ± 111	-100 ± 112	1.01	0.89
A1837 ...	-233 ± 113	-194 ± 156	2.05	1.24
	-206 ± 119	-182 ± 140	1.72	1.30
A1927 ...	436 ± 89	429 ± 107	4.87	3.99
	-93 ± 372	305 ± 244	0.25	1.25
A2029 ...	217 ± 163	258 ± 165	1.33	1.56
	234 ± 169	280 ± 171	1.38	1.63
A2052 ...	-296 ± 90	-221 ± 92	3.28	2.39
	-269 ± 81	-251 ± 83	3.30	3.02
A2063 ...	-147 ± 78	-158 ± 80	1.87	1.96
	-203 ± 91	-234 ± 93	2.23	2.51
A2067 ...	-125 ± 73	-97 ± 77	1.70	1.25
	-157 ± 86	-148 ± 84	1.82	1.76
A2079 ...	-1024 ± 204	-228 ± 93	5.01	2.45
	-202 ± 100	-177 ± 105	2.02	1.68
A2089 ...	142 ± 95	44 ± 89	1.49	0.49
	47 ± 87	32 ± 96	0.54	0.33
A2107 ...	270 ± 86	266 ± 86	3.11	3.07
	270 ± 86	266 ± 86	3.11	3.07
A2124 ...	129 ± 111	130 ± 126	1.16	1.03
	115 ± 113	104 ± 130	1.01	0.80
A2199 ...	258 ± 69	279 ± 72	3.71	3.83
	310 ± 71	346 ± 73	4.33	4.71
A2634 ...	-245 ± 96	-216 ± 96	2.53	2.24
	-300 ± 98	-260 ± 98	3.04	2.64
A2666 ...	141 ± 87	53 ± 84	1.62	0.63
	-74 ± 55	-48 ± 60	1.33	0.80
A2670 ...	410 ± 111	418 ± 115	3.67	3.63
	433 ± 118	390 ± 120	3.66	3.24

NOTE.—For each cluster, the first line gives the cluster properties based on known redshifts within  $3.5 h_{75}^{-1}$  Mpc of the brightest cluster galaxy, and the second line represents the same cluster with the radius restricted to  $1.5 h_{75}^{-1}$  Mpc. Col. (1): cluster name; col. (2) peculiar velocity,  $v_p$ , with respect to the mean cluster velocity, with cosmological correction, and the error in the peculiar velocity with respect to the mean cluster velocity, in kilometers per second; col. (3): peculiar velocity,  $v_{pr}$ , with respect to the biweight location, with cosmological correction and the error in peculiar velocity with respect to the biweight location, in kilometers per second; col. (4): significance,  $S$ , of the peculiar velocity with respect to the mean cluster velocity; col. (5): significance,  $S_r$ , of the peculiar velocity with respect to the biweight location.

Table 3 also lists the significances,  $S$ , following the nomenclature of Sharples et al. (1988) and Hill et al. (1988), where  $S = |v_p|/(\epsilon_{cD}^2 + \epsilon_{cl}^2)^{1/2}$ , and  $\epsilon_{cl}^2 = \sigma_{cl}^2/N_{cl}$ . The robust significance,  $S_r$ , is computed in an analogous manner using  $v_{pr}$  and  $\epsilon_{cl}^2 = S_{bi}^2/N_{bi}$ .

By using the robust significance,  $S_r$ , and restricting the radius to  $1.5 h_{75}^{-1}$  Mpc, only four of the 25 cD galaxies have a significant ( $S_r > 3$ ) measured peculiar velocity—A2052, A2107, A2199, and A2670. Detailed dynamical studies of the four clusters with significant peculiar velocities have been reported by Malumuth et al. (1992; A2052), Oegerle & Hill (1992; A2107), this discussion above (A2199), and Bird (1994; A2670).

A histogram of the measured peculiar velocities of the 25 cD galaxies is shown in Figure 4. The total range of peculiar velocities is quite small, being confined to a value less than  $400 \text{ km s}^{-1}$ . We have analyzed the distribution of robust peculiar velocities,  $v_{pr}$ , reported in Table 3, by treating them as a pseudo-cluster of galaxies. These 25 peculiar velocities were then analyzed with the same suite of dynamical analysis tools that were used to analyze the individual clusters. The mean absolute deviation of the distribution of peculiar velocities is  $168 \text{ km s}^{-1}$ . The observed distribution appears rather flat, and is non-Gaussian according to the  $I$  statistic test. We find that the distribution of peculiar velocities has a biweight location of  $42 \pm 33 \text{ km s}^{-1}$ , which is consistent with zero net velocity, as one would expect for the radial (projected) distribution of any set of galaxies drawn randomly from a sample of clusters. The biweight scale of the distribution of peculiar velocities is  $204 \text{ km s}^{-1}$ , but it decreases to  $164_{-34}^{+41} \text{ km s}^{-1}$  when corrected for the measurement uncertainties reported in Table 3. We interpret this as a significant detection of a velocity dispersion of central cD galaxies around their individual cluster mean velocities.

These results refute the traditional hypothesis that cD galaxies lie exactly at rest in their cluster potential wells, assuming that the clusters are virialized. However, the same results confirm that cD galaxies have a substantially lower velocity than the typical galaxies in their clusters. The biweight scale of  $164 \text{ km s}^{-1}$  in cD peculiar velocities is much less than the mean biweight scale,  $869 \text{ km s}^{-1}$ , for the clusters in this sample.

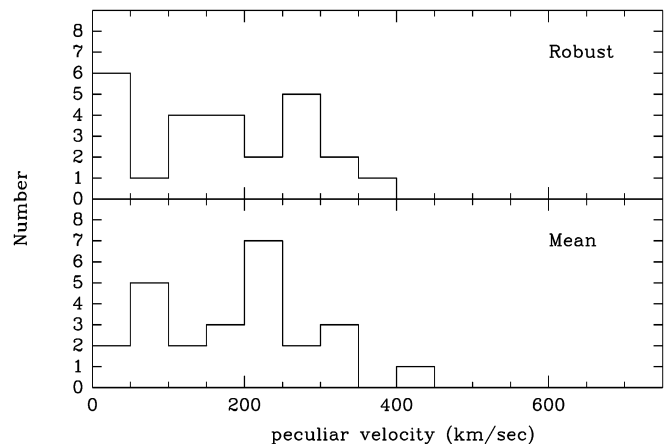


FIG. 4.—Histograms of the distribution of absolute values of peculiar velocities of the cD galaxies in the 25 clusters using galaxies within  $1.5 h_{75}^{-1}$  Mpc of the cluster center. *Top*, peculiar velocity,  $v_{pr}$ , relative to the robust biweight location,  $C_{bi}$ , of the cluster; *bottom*, peculiar velocity,  $v_p$ , relative to the cluster mean velocity.

Peculiar velocities of cD galaxies and our interpretation of them must be scrutinized carefully, since there are a number of subtle and not so subtle effects, which can drastically alter their true value. Furthermore, the root physical cause of a peculiar velocity may not be evident in the kinematical information. Below, we discuss several of these effects.

#### 4.1. Measurement Errors

Whether or not a peculiar velocity is significant depends on the velocity measurement errors for the cD galaxy and on the uncertainty in the mean velocity of the cluster as influenced by the finite number of galaxies measured and the cluster velocity dispersion. Repeated observations of the cD galaxies in our sample have allowed us to measure their velocities fairly accurately. Typical uncertainties for the cD velocities are  $\sim 30 \text{ km s}^{-1}$ . Hence, for a given individual cluster, the measurement error is dominated by the uncertainty in the mean velocity of the cluster, which scales as  $\sigma_{cl}/(N_{cl})^{1/2}$ , typically  $\sim 70\text{--}100 \text{ km s}^{-1}$ . We can then see that, to maintain constant measurement errors for a sample of clusters, it is more difficult to measure a statistically significant peculiar velocity in a high-dispersion cluster, since the number of cluster member velocities that must be determined goes up as the square of the dispersion. This is illustrated in Figure 5, which shows the absolute value of the robust peculiar velocity plotted against the robust dispersion (biweight scale),  $S_{bi}$ , of the cluster. The error bars on the points reflect the uncertainties in the peculiar velocity and the biweight scale, respectively. The clusters with larger dispersions have larger uncertainties in  $C_{bi}$ , and thus it is more difficult to measure a significant peculiar velocity in those clusters.

#### 4.2. Substructure

Substructure can affect the mean cluster velocity and velocity dispersion and hence affect the computed peculiar velocity of the cD. What we really desire to know is whether or not the cD galaxy has a peculiar velocity with respect to the bottom of the potential well of the cluster. Substructure in the core of a cluster can obviously result in a peculiar velocity of the central galaxy. Small subclusters at relatively large distances from the cluster core are dynamically unimportant to the motion of the cD galaxy. However, their inclusion can sometimes substantially alter the computed mean cluster velocity. This can then produce a false signal

of peculiar velocity of the cD galaxy with respect to the cluster.

If we consider all the measured galaxies within  $3.5 h_7^{-1}$  Mpc of the cDs in our sample, then the cDs in clusters A1927, A2052, A2079, A2107, A2199, A2634 and A2670 all have an apparently significant peculiar velocity relative to the cluster mean velocity. This should be compared with the result reported above that only four clusters had cDs with peculiar velocities when galaxies within  $1.5 h_7^{-1}$  Mpc were used in the analysis. These four clusters each have 68 or more member velocities within  $1.5 h_7^{-1}$  Mpc, so the different results obtained within these two radii are not principally due to decreased statistical uncertainty. Clearly, the success with which we are able to sort out spatial and velocity outliers from the projected cluster distribution has a large effect on the computed peculiar velocities of cDs.

We note an apparent absence of cDs with large peculiar velocities in the low-dispersion clusters (see Fig. 5). If cD galaxies form in low-mass groups, which then merge with more massive clusters, then we might expect to find just as many cD galaxies with peculiar velocities in low-mass clusters as in higher mass clusters. Alternately, if cDs form in low-velocity dispersion groups and have time to come to rest in that potential well, then we might expect them to have smaller peculiar velocities in that environment and large peculiar velocities after the merger into the larger cluster. This is very difficult to evaluate because poor groups and clusters do not have enough galaxies in them to give a good measurement of the mean cluster velocity. However, the small number of low-mass (low dispersion) clusters in this sample is not adequate to address this issue.

In Figure 6, we have plotted the fraction of simulated clusters containing more apparent substructure than the observed cluster,  $f(\Delta_{sim} > \Delta_{obs})$ , against the robust significance,  $S_r$ . We see that three of the four clusters with  $S_r > 3$  show small values of  $f$ , implying that they have statistically significant substructure as detected by the Dressler-Shectman test. Not all varieties of substructure are necessarily detected by the Dressler-Shectman test, so substructure could account for all the significant peculiar velocities that we observe. See Pinkney et al. (1996) for a summary of the various statistical tests available to study substructure. Alternately, the absence of clusters in the upper right corner of Figure 6 indicates that clusters without substructure do not have cDs with significant peculiar velocities.

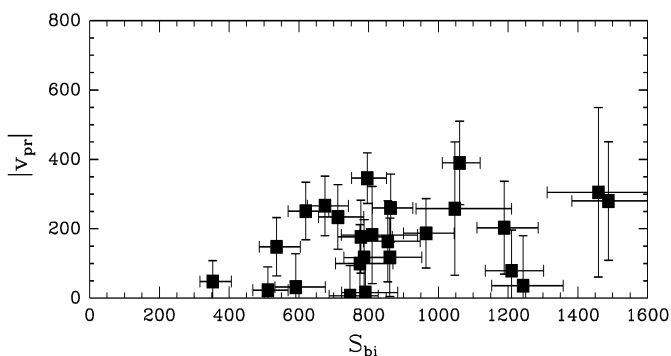


FIG. 5.—Absolute value of the robust peculiar velocity,  $v_{pr}$ , plotted against the biweight scale,  $S_{bi}$ , for 25 clusters, using galaxies within  $1.5 h_7^{-1}$  Mpc of the cluster center.

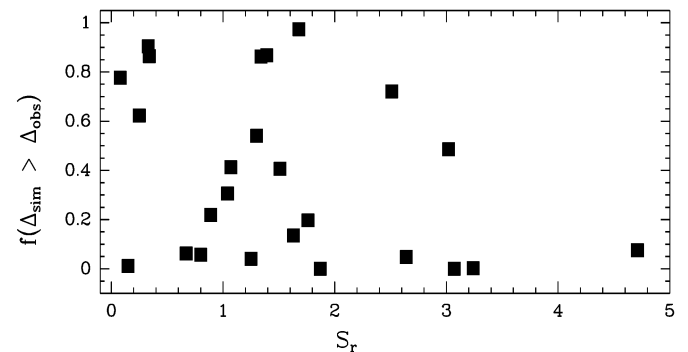


FIG. 6.—Fraction of 1000 simulated clusters (for each real cluster) with  $\Delta_{sim} > \Delta_{obs}$  from the Dressler-Shectman test, plotted against the robust significance,  $S_r$ , of the peculiar velocity for 25 clusters, using galaxies within  $1.5 h_7^{-1}$  Mpc of the cluster center.

Mergers of subclusters and groups into a massive cluster also have the possibility to disturb a cD galaxy from its resting place at the bottom of the potential well. Zabludoff & Zaritsky (1995) present observations of the cluster A754 that they argue is the result of a collision between two subclusters. While this is an extreme example, it serves to illustrate that mergers can disrupt the location and/or velocity of a cD galaxy. Smaller mergers would be expected several times during the lifetime of a cluster. Pinkney et al. (1993) suggest that such a merger could have resulted in the peculiar velocity of the cD galaxy in A2634, although that peculiar velocity is only marginally significant. Bird (1994) also reports evidence for two or more subclusters in A2670 that may be the remnants of the groups that formed the rich cluster.

#### 4.3. Galaxy Mergers and Interactions with the cD

cD galaxies often contain multiple nuclei that potentially can exert a gravitational influence on the primary nucleus, either through mergers or by dynamical interactions. Hoessel (1980) finds that 28%–45% of BCGs contain secondary nuclei within  $10 h_{75}^{-1}$  kpc of the center of the BCG, which is too high a fraction to be explained by chance superposition. Lauer (1988) has performed a photometric study of the light profiles of 16 multiple nucleus BCGs and found evidence for interactions between the multiple nuclei and the BCG in about half the cases. In many cases, these nuclei are moving through the cluster core too rapidly to merge with the BCG. Lauer (1990) suggests that only 25% of the multiple nuclei systems are currently merging with the BCG.

Consider the effects of a high-speed encounter of a galaxy of mass  $m_g$  moving through the cluster core with velocity  $v_g$ . The impulse approximation will hold for passage within a distance  $b = r_{cD} v_g / \sigma_{cD}$  of the cD galaxy, where  $r_{cD}$  and  $\sigma_{cD} \approx (G m_{cD} / r_{cD})^{1/2}$  are the radius and velocity dispersion of the cD galaxy, respectively. The perpendicular velocity component of the impulse, which is substantially larger than the parallel component, is given by

$$\delta v = \frac{2m_g b v_g^3}{G(m_{cD} + m_g)^2} \left[ 1 + \frac{b^2 v_g^4}{G^2(m_{cD} + m_g)^2} \right]^{-1}$$

(Binney & Tremaine 1987). The second factor above is  $\gg 1$ , so that  $\delta v \approx 2Gm_g/bv_g$ . If we assume that the perturbing galaxy's mass has been tidally truncated with a value given by  $m_g/m_{cD} \approx (\sigma_g/\sigma_{cD})^3$  and  $b = r_{cD} v_g / \sigma_{cD}$ , we then derive the result  $\delta v \approx 2\sigma_g^3/v_g^2$ . With values  $v_g = 1000 \text{ km s}^{-1}$  and  $\sigma_g = 200 \text{ km s}^{-1}$ , the velocity kick imparted to the cD is  $\sim 16 \text{ km s}^{-1}$ . On average, the observed (projected) peculiar velocity would be  $\delta v/\sqrt{3} \sim 10 \text{ km s}^{-1}$ . Even this relatively small velocity kick will decay fairly quickly because of dynamical friction. Lauer (1988) derives the characteristic decay time of this velocity to be  $\approx 0.5t_c$ , where  $t_c$  is the crossing time of the perturbing galaxy. For representative impact parameters and velocities, the decay time is  $\sim 10^8 \text{ yr}$ . Hence, perturbations in the velocity of the cD nucleus will be damped out fairly quickly, and furthermore, there will be only of order one high-speed encounter per crossing time. We conclude that velocity “kicks” due to galaxies passing through the cluster core are very unlikely to explain the peculiar velocities that are observed.

Malumuth (1992) has simulated the evolution of galaxy clusters and the formation of cD galaxies by dynamical

friction. He finds that after  $10^{10} \text{ yr}$  only a few percent of central galaxies have projected peculiar velocities larger than  $300 \text{ km s}^{-1}$ . Looking earlier in the simulations at the epoch when the cDs are born roughly doubles the number with large peculiar velocities, but that number is still well below what we observe. We find that our data are still in agreement with Malumuth's conclusion that cDs formed in virialized clusters would have a distribution of peculiar velocities that is inconsistent with (smaller than) the observed distribution.

We have tried to obtain velocities of extra nuclei of the BCGs if they are comparable in brightness (and hence mass) to the primary nucleus. It was not possible to obtain velocities of all multiple nuclei, and hence we have relied on measurements by other authors who have specifically studied multiple nuclei (Tonry 1984, 1985; Hu, Cowie, & Wang 1985; Blakeslee & Tonry 1992).

#### 5. FORMATION SCENARIOS FOR cD GALAXIES

Our question at the beginning of this decade-long dynamical survey of cD clusters of galaxies was whether the number and distribution of cD peculiar velocities would be able to constrain the models of cD formation and growth.

The notion that cD galaxies have formed over a long period of time in the center of a rich cluster of galaxies because of cannibalism or mergers (the postcollapse model) has given way in recent years to the idea that cD galaxies formed long ago prior to cluster collapse and virialization. Merritt (1985) and Lauer (1988) have argued that the large luminosities of cDs cannot be built over a cluster lifetime based on dynamical friction rates. Our observations of substructure seem to support the idea that cD galaxies live in clusters that are dynamically young and not completely virialized.

West (1994) has pointed to the cD “alignment effect” (the fact that cD halos are preferentially elongated in the direction of large-scale structures of galaxies) as evidence that cDs are formed by a process of mergers of clumps of mass that fall anisotropically along preferred axes whose orientations are related to the large-scale density field. In this formation mechanism, cD galaxies are born early in the life of the cluster, as the cluster forms around the cD. Dubinski (1998) has made a detailed cosmological simulation of cluster collapse. He finds that the central galaxy forms through a merger of several massive galaxies in a filament early in the clusters' history. cD galaxies formed in this manner would be expected to lie at the bottom of the potential well, unless late merging of subclusters disrupted the potential well slightly.

Zabludoff & Mulchaey (1998) have argued that cD galaxies form from galaxy-galaxy collisions in poor groups of galaxies, where merger efficiencies are improved by the low group velocity dispersions. These poor groups, with their central massive galaxies, then merge with other poor groups or fall into existing clusters. This model is attractive in that it explains the existence of cD galaxies in relatively poor clusters and provides a natural explanation for the cD peculiar velocities that we observe. However, it is not clear how a cD envelope would survive the tidal shear as it falls into a massive cluster. If all cDs formed initially in poor groups of galaxies and then later merged their way into the center of rich clusters, then a larger sample of clusters might be expected to show a few clusters in which the cDs had very large peculiar velocities. In this sample of 25 clusters, we do

not see any peculiar velocities as large as the cluster velocity dispersion.

## 6. CONCLUSIONS

We have completed a dynamical study of a complete sample of 25 clusters of galaxies with central cD galaxies. Redshifts for galaxies in three of the clusters were obtained from the literature. Redshifts for the other 22 clusters were taken from our own observations combined with velocities from the literature. The number of cluster member galaxies with observed velocities ranged from 38 to 236 per cluster.

We have reported the detailed dynamical results for the 11 clusters for which we presented data in Paper III. In addition, we have recomputed the dynamical properties for all 25 clusters in the sample, using our own data combined with redshifts from the literature. Robust statistical estimators (Beers et al. 1990) of mean cluster velocity and dispersion (biweight location and scale) have been used to carefully assess the significance of our results, which are summarized below.

Of these 25 clusters, four show significant peculiar velocities of the cD galaxies relative to the cluster biweight location (i.e., robust mean velocity), using the criterion that  $S_r > 3$  for galaxies within  $1.5 h_{75}^{-1}$  Mpc of the cD. Those clusters are A2052, A2107, A2199, and A2670, with peculiar velocities between 250 and 400 km s<sup>-1</sup>. The distribution of all cD peculiar velocities in our sample has a biweight scale (i.e., robust dispersion) of  $164_{-34}^{+41}$  km s<sup>-1</sup>, indicating that cD galaxies are not strictly at rest with respect to the potential wells of their parent clusters.

We confirm the existence of peculiar velocities of cD galaxies relative to the mean velocity of their clusters. However, cD peculiar velocities and their dispersion are significantly lower than the velocity dispersions of the cluster galaxies in the survey, making them kinematically distinct from the rest of the cluster population. Therefore, we also confirm the traditional view that cD galaxies are approximately at rest in their cluster potential well.

Having established the statistical reality of cD peculiar velocities, we have considered the origin of these velocities. Various authors (Hill et al. 1988; Malumuth 1992) have explored galaxy-galaxy interactions and multiple nuclei in the vicinity of the cD as the causes of the peculiar velocities. However, the amplitudes and frequency of the observed peculiar velocities are greater than expected.

Of the 25 clusters surveyed here, eight (~30%) show evidence of subclustering at the 90% confidence level [i.e.,  $f(\Delta_{\text{sim}} > \Delta_{\text{obs}}) < 0.1$ ] when considering galaxies within  $1.5 h_{75}^{-1}$  Mpc of the cluster center. When the cluster radius is

extended to  $3.5 h_{75}^{-1}$  Mpc 13 clusters (~50%) in the survey show evidence of substructure. This level of subclustering is in good agreement with that reported by other investigations using optical or X-ray surveys (Geller & Beers 1982; Dressler & Shectman 1988; West, Jones, & Forman 1995; Solanes, Salvador-Solé, & González-Casado 1999). From this we conclude that cD clusters are dynamically no different than other present-day clusters of the same richness. Furthermore, since dynamical evolution would be expected to erase substructure within several cluster crossing times, the presence of subclustering indicates that cD clusters are still evolving.

Substructure in these clusters appears to be the cause of the observed cD peculiar velocities. Of the four clusters with significant cD peculiar velocities, three have significant subclustering (see Fig. 6). As the clusters continue to form, subclusters fall into the parent cluster, thereby modifying the cluster potential well. This process could allow the cD galaxy to remain nearly at rest in its local environment while still having a mild peculiar velocity relative to the cluster as a whole.

Our dynamical data reported above do not lead us to a definite conclusion about the formation mechanism of cD galaxies. However, we now have better observational constraints to place on those models. Whether formed in situ or elsewhere, present-day cD galaxies must be nearly at rest with respect to the cluster potential but not exactly at rest. The small peculiar velocity of the cD galaxies may be either a residual effect from their formation or the result of recent interactions and mergers of the cluster as a whole. Future kinematic studies of cD clusters at high redshift may provide the necessary clues to the origin of cD galaxies.

This work was partially supported by NASA through grant NAGW-2988 to W. R. O. at Johns Hopkins University, and NICMOS GTO grant NAG 5-3042 to J. M. H. at the University of Arizona. Oegerle would like to acknowledge the hospitalities of Steward Observatory and Kitt Peak National Observatory during visits when much of this paper was written.

We thank John Huchra for supplying us with up-to-date versions of ZCAT (Huchra et al. 1992) for the cross-referencing of velocities in the literature, Tina Bird for providing a digital version of the A2670 velocities published by Sharples et al. (1988), and Oleg Gnedin for helpful comments. This research has also made use of the NASA/IPAC Extragalactic Database, which is operated by the Jet Propulsion Laboratory, California Institute of Technology, under contract with NASA.

## REFERENCES

- Beers, T. C., Flynn, K., & Gebhardt, K. 1990, *AJ*, 100, 32  
 Binney, J., & Tremaine, S. 1987, in *Galactic Dynamics*, ed. J. P. Ostriker (Princeton: Princeton Univ. Press)  
 Bird, C. 1994, *ApJ*, 422, 480  
 Blakeslee, J. P., & Tonry, J. L. 1992, *AJ*, 103, 1457  
 Dressler, A., & Shectman, S. 1988, *AJ*, 95, 985  
 Dubinski, J. 1998, *ApJ*, 502, 141  
 Geller, M., & Beers, T. 1982, *PASP*, 94, 421  
 Gregory, S. A., & Thompson, L. A. 1984, *ApJ*, 286, 422  
 Hausman, M. A., & Ostriker, J. P. 1978, *ApJ*, 224, 320  
 Hill, J. M., Hintzen, P., Oegerle, W. R., Romanishin, W., Lesser, M. P., Eisenhamer, J. D., & Batuski, D. J. 1988, *ApJ*, 332, L23  
 Hill, J. M., & Oegerle, W. R. 1993, *AJ*, 106, 831 (Paper I)  
 ———, 1998, *AJ*, 116, 1529 (Paper III)  
 Hoessel, J. G. 1980, *ApJ*, 241, 493  
 Hoessel, J. G., Gunn, J. E., & Thuan, T. X. 1980, *ApJ*, 241, 486 (HGT)  
 Hu, E. M., Cowie, L. L., & Wang, Z. 1985, *ApJS*, 59, 447  
 Huchra, J., Geller, M., Clemens, C., Tokarz, S., & Michel, A. 1992, *Bull. Inf. CDS*, 41, 31  
 Jones, C., Mandel, E., Schwarz, J., Forman, W., Murray, S. S., & Harnden, F. R. 1979, *ApJ*, 234, L21  
 Krempeč-Krygier, J., & Krygier, B. 1999, *Acta Astron.*, 49, 403  
 Lauer, T. 1988, *ApJ*, 325, 49  
 ———, 1990, in *Dynamics and Interactions of Galaxies*, ed. R. Wielen (Heidelberg: Springer), 406  
 Malumuth, E. M. 1992, *ApJ*, 386, 420  
 Malumuth, E. M., Kriss, G. A., Van Dyke Dixon, W., Ferguson, H. C., & Ritchie, C. 1992, *AJ*, 104, 495  
 Matthews, T. A., Morgan, W. W., & Schmidt, M. 1964, *ApJ*, 140, 35  
 Merritt, D. 1985, *ApJ*, 289, 18  
 Oegerle, W. R., & Hill, J. M. 1992, *AJ*, 104, 2078  
 ———, 1994, *AJ*, 107, 857  
 Oegerle, W. R., Hill, J. M., & Fitchett, M. J. 1995, *AJ*, 110, 32  
 Owen, F. N., & Eilek, J. A. 1998, *ApJ*, 493, 73

- Pinkney, J., Rhee, G., Burns, J. O., Hill, J. M., Oegerle, W., Batuski, D., & Hintzen, P. 1993, *ApJ*, 416, 36
- Pinkney, J., Roettiger, K., Burns, J. O., & Bird, C. M. 1996, *ApJS*, 104, 1
- Quintana, H., & Lawrie, D. G. 1982, *AJ*, 87, 1
- Scodreggio, M., Solanes, J. M., Giovanelli, R., & Haynes, M. P. 1995, *ApJ*, 444, 41
- Sharples, R. M., Ellis, R. S., & Gray, P. M. 1988, *MNRAS*, 231, 479
- Siddiqui, H., Stewart, G. C., & Johnstone, R. M. 1998, *A&A*, 334, 71
- Small, T. A., Ma, C.-P., Sargeant, W. L. W., & Hamilton, D. 1998, *ApJ*, 492, 45
- Small, T. A., Sargeant, W. L. W., & Hamilton, D. 1997, *ApJS*, 111, 1
- Solanes, J. M., Salvador-Solé, E., & González-Casado, G. 1999, *A&A*, 343, 733
- Struble, M. F., & Rood, H. J. 1987, *ApJS*, 63, 555
- Teague, P., Carter, D., & Gray, P. 1990, *ApJS*, 72, 715
- Tonry, J. L. 1984, *ApJ*, 279, 13
- . 1985, *AJ*, 90, 2431
- West, M. J. 1994, *MNRAS*, 268, 79
- West, M. J., Jones, C., & Forman, W. 1995, *ApJ*, 451, L5
- Yahil, A., & Vidal, N. V. 1977, *ApJ*, 214, 347
- Zabludoff, A. I., & Mulchaey, J. S. 1998, *ApJ*, 496, 39
- Zabludoff, A. I., & Zaritsky, D. 1995, *ApJ*, 447, L21